

# Anisotropies in insulating $\text{La}_{2-x}\text{Sr}_x\text{CuO}_4$ : angular resolved photoemission and optical absorption

O. P. Sushkov,<sup>1</sup> Wenhui Xie,<sup>2</sup> O. Jepsen,<sup>2</sup> O. K. Andersen,<sup>2</sup> and G. A. Sawatzky<sup>3</sup>

<sup>1</sup>*School of Physics, University of New South Wales, Sydney 2052, Australia*

<sup>2</sup>*Max-Planck-Institut für Festkörperforschung, Heisenbergstrasse 1, D-70569 Stuttgart, Germany*

<sup>3</sup>*Department of Physics and Astronomy, University of British Columbia, Vancouver B. C. V6T-1Z1, Canada*

Due to the orthorhombic distortion of the lattice, the electronic hopping integrals along the  $a$  and  $b$  diagonals, the orthorhombic directions, are slightly different. We calculate their difference in the LDA and find  $t'_a - t'_b \approx 8$  meV. We argue that electron correlations in the insulating phase of  $\text{La}_{2-x}\text{Sr}_x\text{CuO}_4$ , i. e. at doping  $x \leq 0.055$ , dramatically enhance the  $(t'_a - t'_b)$ -splitting between the  $a$ - and  $b$ -hole valleys. In particular, we predict that the intensity of both angle-resolved photoemission and of optical absorption is very different for the  $a$  and  $b$  nodal points.

## INTRODUCTION

The magnetic state of  $\text{La}_{2-x}\text{Sr}_x\text{CuO}_4$  (LSCO) changes tremendously with Sr doping. The three-dimensional antiferromagnetic Néel order identified [1] below 325 K in the parent compound disappears at doping  $x \approx 0.02$  and gives way to the so-called spin-glass phase which extends up to  $x \approx 0.055$ . In both, the Néel and the spin-glass phase, the system essentially behaves as an Anderson insulator and exhibits only hopping conductivity [1, 2]. Superconductivity then sets in for doping  $x \gtrsim 0.055$ , see Ref. 1. One of the most intriguing properties of LSCO is the static incommensurate magnetic order observed at low temperature in elastic neutron scattering experiments. This order manifests itself as a scattering peak shifted with respect to the antiferromagnetic position. Very importantly, the incommensurate order is a generic feature of LSCO. According to experiments in the Néel phase, the incommensurability is almost doping independent and directed along the orthorhombic  $b$  axis [3]. In the spin-glass phase, the shift is also directed along the  $b$  axis, but scales linearly with doping [4, 5, 6]. Finally, in the underdoped superconducting region ( $0.055 \lesssim x \lesssim 0.12$ ), the shift still scales linearly with doping, but it is directed along the crystal axes of the tetragonal lattice [7]. In the present work we discuss only the insulating phase,  $x \leq 0.055$ . It is clear that pinning of the diagonal spin structure is due to the orthorhombic distortion of the crystal. A mechanism for pinning of the diagonal spin structure to the orthorhombic  $b$  axis was suggested in Refs. [8, 9, 10]. The mechanism has four components:

1) Due to strong antiferromagnetic correlations, the minima of dispersion of a mobile hole are at points  $(\pm\pi/2, \pm\pi/2)$  of the Brillouin zone, so the system can, to some extent, be considered as a two valley semiconductor.

2) At low temperature, each hole is trapped in a hydrogen-like bound state near the corresponding Sr ion, the binding energy is about 10 meV and the radius of the bound state is about 10 Å.

3) Due to the orthorhombic distortion, the diagonal hopping matrix elements  $t'_a$  and  $t'_b$  are slightly different, and this makes the  $b$  valley,  $(-\pi/2, \pi/2)$ , deeper than the  $a$  valley,  $(\pi/2, \pi/2)$ . So all the hydrogen-like bound states are built with holes from the  $b$ -valley.

4) Each hydrogen like bound state creates a spiral distortion of the spin background and the distortion is observed in neutron scattering. So the state at  $0.02 < x < 0.055$  is not a spin glass, it is a disordered spin spiral.

In the present paper we calculate accurately the diagonal hopping matrix elements and show that the difference is  $t'_a - t'_b \approx 8$  meV. We also discuss the implications of the described physics for the  $p^5d^9 \rightarrow p^6d^8$  optical absorption and for angle-resolved photoemission (ARPES). The optical absorption probes the charge distribution, and we predict that the absorption vanishes for polarization along the orthorhombic  $a$ -direction. ARPES probes the spin spiral, and we predict very different spectra in  $a$  and  $b$  nodal points.

## ANISOTROPY OF $t'$ DUE TO ORTHORHOMBIC DISTORTION AND TILTING

The 2D  $t - J$  model was suggested two decades ago to describe the essential low-energy physics of high- $T_c$  cuprates [11, 12, 13]. In its extended version, this model includes additional hopping matrix elements  $t'$  and  $t''$  to respectively 2nd and 3rd-nearest Cu neighbors. The Hamiltonian of the  $t - t' - t'' - J$  model on the square Cu lattice has the form:

$$H = -t \sum_{\langle ij \rangle \sigma} c_{i\sigma}^\dagger c_{j\sigma} + t' \sum_{\langle ij' \rangle \sigma} c_{i\sigma}^\dagger c_{j'\sigma} - t'' \sum_{\langle ij'' \rangle \sigma} c_{i\sigma}^\dagger c_{j''\sigma} + J \sum_{\langle ij \rangle \sigma} \left( \mathbf{S}_i \mathbf{S}_j - \frac{1}{4} n_i n_j \right). \quad (1)$$

Here,  $c_{i\sigma}^\dagger$  is the creation operator for an electron with spin  $\sigma$  ( $\sigma = \uparrow, \downarrow$ ) at site  $i$  of the square lattice,  $\langle ij \rangle$  indicates 1st-,  $\langle ij' \rangle$  2nd-, and  $\langle ij'' \rangle$  3rd-nearest neighbor sites. The spin operator is  $\mathbf{S}_i = \frac{1}{2} c_{i\alpha}^\dagger \boldsymbol{\sigma}_{\alpha\beta} c_{i\beta}$ , and  $n_i = \sum_{\sigma} c_{i\sigma}^\dagger c_{i\sigma}$

with  $\langle n_i \rangle = 1 - x$  being the number density operator. In addition to the Hamiltonian (1) there is the constraint of no double occupancy, which accounts for strong electron correlations. The values of the parameters of the Hamiltonian (1) for LSCO are known from neutron scattering [1], Raman spectroscopy [14], and ab-initio calculations [15] to be:

$$\begin{aligned} J &\approx 140 \text{ meV}, & t &\approx 450 \text{ meV}, \\ t' &\approx 70 \text{ meV}, & t'' &\approx 35 \text{ meV}. \end{aligned} \quad (2)$$

Note that the signs of the hopping terms in the electron Hamiltonian (1) have been chosen in such a way that, for a  $d_{x^2-y^2}$  orbital, the hopping matrix elements are positive.

The dispersion of the hole dressed by magnetic quantum fluctuations has minima at the nodal points  $\mathbf{q}_0 = (\pm\pi/2, \pm\pi/2)$  and is practically isotropic in the vicinity of each [9]:

$$\begin{aligned} \epsilon(\mathbf{q}) &\approx \epsilon(\mathbf{q}_0) + \frac{1}{2}\beta(\mathbf{q} - \mathbf{q}_0)^2 \\ \beta &\approx 2J \approx 260 \text{ meV}. \end{aligned} \quad (3)$$

We set the lattice spacing to unity,  $3.81 \text{ \AA} \rightarrow 1$ . The effective mass corresponding to the quadratic dispersion (3) is approximately twice the electron mass.

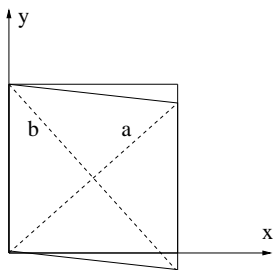


FIG. 1: Orthorhombic deformation of the square lattice

In the low-temperature orthorhombic (LTO) phase, the square Cu lattice is slightly deformed as indicated in Fig. 1: The angles,  $\pi/2 \pm \varphi$ , between the edges are obtuse or acute, such that the  $(11)$  and  $(1-1)$  diagonals, the orthorhombic translations, have slightly different lengths, respectively  $a = \sqrt{2}(1 - \varphi/2)$  and  $b = \sqrt{2}(1 + \varphi/2)$ . On top of this comes an alternating tilt of the oxygen octahedra around the  $a$  axis by an angle  $\pm\theta$ , whereby the oxygens in the layer buckle out of the Cu plane forming a  $[-\pi/2, \pi/2]$ -wave in the  $b$ -direction [1, 16]. The values of the orthorhombic and tilting deformations,

$$\varphi = 0.009 \text{ (} 0.5^\circ \text{)} \quad \text{and} \quad \theta = 0.05 \text{ (} 3^\circ \text{)}, \quad (4)$$

are so tiny that they hardly influence  $J$ ,  $t$  and  $t''$ , but they do make the diagonal hopping significantly different in the  $a$  and  $b$  directions, as we show below. Including

$t'_a \neq t'_b$  in the first, one-electron part of the Hamiltonian (1) yields the following 2D bandstructure:

$$\begin{aligned} \epsilon(\mathbf{k}) &= -2t(\cos k_x + \cos k_y) - 2t''(\cos 2k_x + \cos 2k_y) \\ &\quad + 2t'_a \cos(k_x + k_y) + 2t'_b \cos(k_x - k_y). \end{aligned} \quad (5)$$

Note that  $\epsilon$  denotes electron energies and  $\epsilon$  hole energies. The splitting of the bare valleys is:

$$\begin{aligned} \epsilon(-\pi/2, \pi/2) - \epsilon(\pi/2, \pi/2) &\equiv \epsilon_b - \epsilon_a \\ &= 4(t'_a - t'_b) \equiv 4\delta t'. \end{aligned} \quad (6)$$

For comparison, we show in the left-hand side of Fig. 2 the bandstructure calculated from density-functional theory (LDA) along the lines connecting the high-symmetry points  $\Gamma$   $(0, 0, 0)$ , R  $(\pi, 0, \pi/2)$ , S  $(\pi/2, \pi/2, \pi/2)$ , Y  $(0, 0, \pi/2)$ , and B  $(-\pi/2, \pi/2, \pi/2)$  of the 3D *orthorhombic* (*Bmab*) Brillouin zone (BZ). For simplicity, we have given the coordinates in terms of the nearly *tetragonal* reciprocal Cu-lattice translations.  $k_z = \pi/2$  is halfway to the Brillouin-zone boundary where the influence of inter-layer hopping is minimal. We see that no gapping is caused by the  $[-\pi/2, \pi/2]$  tilting wave. As a consequence, the LDA bandstructure may be folded out to the nearly tetragonal BZ where expression (5) adequately represents the dispersion of the LDA conduction band, indicated by heavy lining, near half-filling. On the right-hand side of Fig. 2 we show a blow-up of the orthorhombic LDA bands near the nodal points, S  $(\pi/2, \pi/2, \pi/2)$  and B  $(\pi/2, -\pi/2, \pi/2)$ , along the respective nodal direction,  $a$  and  $b$ . Finally we see that two different computational techniques, LMTO and LAPW, give essentially the same result, namely

$$\delta t' \approx 8 \text{ meV}, \text{ i.e. } \delta t'/t' \approx 11\%. \quad (7)$$

This number is surprisingly large: Had the Cu  $d_{x^2-y^2}$  conduction-band Wannier-like orbital been a simple, canonical orbital [21], the hopping between two such orbitals would have decreased as their distance to the power  $-(l+l'+1)$ , which for two  $d$  orbitals is  $-5$ , and, hence,  $\delta t'/t' = 5\varphi = 4.5\%$ . This, however, neglects that the hopping is almost exclusively via the  $O_x p_x$  and  $O_y p_y$  orbitals, as is amply demonstrated by an LDA calculation in which we took the tilting wave to run along  $a$  instead of along  $b$ . The result was a four times reduction of  $\delta t'$  compared to (7)! We therefore conclude that tilting is almost as important as orthorhombicity for the hopping anisotropy.

To understand why, we turn to the simplest model showing an effect of tilting: Emery's 3-band model [12] which keeps merely the  $t_{pd}$  hopping between Cu  $d_{x^2-y^2}$  and its nearest  $O_x p_x$  and  $O_y p_y$  orbitals, as well as the  $t_{pp}$  hopping between the nearest  $O_x p_x$  and  $O_y p_y$  neighbors. It is easy to see that in this model,

$$t' = 2 \frac{t_{pd} t_{pp} t_{pd}}{(\epsilon_F - \epsilon_p)^2}, \text{ so that } \frac{\delta t'}{t'} = \frac{\delta t_{pp}}{t_{pp}} \quad (8)$$

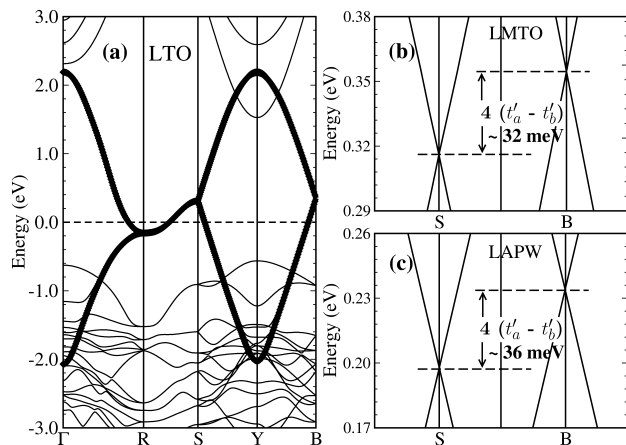


FIG. 2: LDA bandstructure of the LTO phase shown in the orthorhombic BZ (see text). (a) NMTO downfolded Cu  $d_{x^2-y^2}$  - like conduction bands shown in thick lines [18]. (b) Blow-up of conduction bands near the nodal points S and B, and along the respective nodal lines,  $a$  and  $b$ . (c) same as (b), but calculated with the full-potential Linear Augmented Plane Wave Method (LAPW) [20] instead of the Linear Muffin Tin Orbital Method (LMTO) [19]

because  $t_{pd}$  and the distance of the O  $p$  level,  $\varepsilon_p$ , below the half-filling level,  $\varepsilon_F$ , are not influenced by the deformations. In the deformed structure, each plane oxygen remains midway between its two nearest Cu neighbors, but is slightly above or below the Cu plane. Moreover, the O  $p$  orbital is parallel to the Cu-Cu line, so that the two O  $p$  orbitals via which the  $t'_{a/b}$  hopping takes place are at the acute/obtuse angle  $\pi/2 \mp \varphi$ . The main effect of the deformation is, however, not this misalignment, but simply that the distance between the oxygens at the acute angle is  $a/2$  and that between the oxygens at the obtuse angle is  $b/2/\cos\theta$ . With  $l = l' = 1$ , this gives:  $\delta t'/t' = 3(\varphi + \theta^2) = 3(0.90 + 0.25)\% \approx 3.5\%$ , which, due to the slower decay of canonical  $p$  orbitals, is even smaller than the previous  $dd$  estimate. Also the tilting contribution is too small. Inclusion of the orbital misalignments in the canonical approximation [21] merely changes the result to:  $\delta t'/t' = \frac{7}{3}\varphi + 5\theta^2 \approx (2.1 + 1.3)\% = 3.4\%$ .

Another simple model is the axial-orbital model [15] which adds to the three orbitals of the Emery model a Cu-centered, axial orbital, but keeps only hops between nearest neighbors: from O  $p$  to Cu  $d_{x^2-y^2}$  ( $t_{pd}$ ) and to the axial orbital ( $t_{sp}$ ). The axial orbital is a hybrid between Cu  $4s$ , Cu  $3d_{3z^2-1}$ , apical O  $p_z$  and axial cation orbitals, and its energy,  $\varepsilon_s$  ( $> \varepsilon_F$ ) is the material dependent electronic parameter in the LDA. Since  $t_{pp}$  proceeds via the axial orbital in this model, and therefore equals  $t_{4sp}^2/(\varepsilon_s - \varepsilon_F)$ , it cannot depend on  $\varphi$ ! For the same reason, the hopping from O  $x p_x$  to O  $x p_x$  over the distance 1 has the same value,  $t_{pp}$ , and this is what leads to  $t'' = t'/2$  when downfolding to the 1-band model [15].

However, recent first-principles 3-band Hamiltonians formed by numerical downfolding of the LDA Hilbert space [18] do not support this; they yield a  $p_x$ - $p_x$  hop, which can only be understood by the presence of a large material-independent contribution,  $-t_{4pp}^2/(\varepsilon_{4p} - \varepsilon_F)$ , from hopping via Cu  $4p_x$  [22]. To the  $p_x$ - $p_y$  hop, there can be no such contribution, - *unless* there is orthorhombic distortion. Also buckling-induced anisotropy may be caused by hopping via Cu  $4p_z$ .

To see whether coupling via excited Cu  $4p$  degrees of freedom can be the reason for the surprisingly large anisotropy (7) found by the LDA calculations, we now add these degrees of freedom to the axial model and, as usual, include hops only between nearest neighbors. For the directional dependences we use the canonical approximation and find:

$$\begin{aligned} \frac{\delta t'}{t'} = \frac{\delta t_{pp}}{t_{pp}} &= (2\varphi + 4.5\theta^2) \left( \frac{t_{4pp}}{t_{sp}} \right)^2 \frac{\varepsilon_s - \varepsilon}{\varepsilon_{4p} - \varepsilon} \\ &\approx (1.8 + 1.1)\% \times \left( \frac{2.6}{2.3} \right)^2 \frac{35}{11} = 12\%. \end{aligned}$$

The superb agreement with the LDA result (7) may be fortuitous, but also the relative contribution from orthorhombicity and tilt agrees. So we believe that the surprisingly large hopping anisotropy to be explained by this simple expression. It may be noted that going to materials with higher  $T_{c\max}$ ,  $\varepsilon_s$  decreases and with it the hopping anisotropy. Finally it should be noted that for simplicity we have taken  $\varepsilon_{4z} = \varepsilon_{4p}$  ( $\equiv \varepsilon_{4x/y}$ ), although  $\varepsilon_{4z}$  is an axial orbital and, hence, material dependent.

The  $t'$  describes hopping within the same magnetic sublattice. Therefore, to account for many electron correlations in the anisotropy of the single hole dispersion one only needs to know the quasiparticle residue  $Z(\mathbf{q})$ . This leads to anisotropic correction to the hole dispersion [9]

$$\delta \varepsilon(\mathbf{q}) = 2Z(\mathbf{q}) \delta t' \sin q_x \sin q_y. \quad (9)$$

The correction to the dispersion vanishes at antinodal points  $(0, \pi)$ ,  $(\pi, 0)$  and it is maximum at nodal points,  $(\pm\pi/2, \pm\pi/2)$ , where  $Z \approx 0.3$ . The energy difference between the nodal points is

$$\varepsilon_a - \varepsilon_b = 4Z\delta t' \sim 10 \text{ meV}. \quad (10)$$

Thus, at low temperature all hydrogen-like bound states are formed from the  $b$ -valley holes, the  $a$ -valley is empty. We would like to stress that this is true only in the insulating phase. In the superconducting phase which arises after percolation of the bound states,  $x > 0.055$ , both valleys are populated.

The energy difference (10) is the single hole effect. It accounts for spin quantum fluctuations, but it assumes usual Neel order. There is another collective contribution to the energy difference  $\varepsilon_a - \varepsilon_b$ . The collective contribution is due to the spiral spin ordering established at

$0.02 \leq x \leq 0.055$ . The collective contribution is considered below in the ARPES section. Certainly, in the end the collective contribution is also driven by the asymmetry (10) because the asymmetry's causes depopulation of the  $a$ -valley.

### IMPLICATIONS FOR OPTICAL TRANSITIONS

$$p^5 d^9 \rightarrow p^6 d^8$$

We consider the optical transitions involving removing a  $d$  electron from a central placket of Fig. 3 resulting in a  $d^8$ -state and transferring it to a linear combination of Zhang Rice (ZR) singlet states on neighboring plackets. Note that the transition staying within the same plaque is not allowed optically. This particular transition is of course only allowed if there is a hole in the ZR state on neighboring plackets and therefore is only present in a hole doped material. In the undoped material the corresponding transition would have to be to neighboring  $d$  states resulting in a linear combination of  $d^{10}$  configurations there. This transition would be at an energy of about the charge transfer gap higher than the transitions to ZR singlet states and is easily distinguishable from those to the ZR states. These transitions involve the full  $d^8$  multiplet structure and their energies can be obtained from the calculations described in Ref. [23] as well as from early resonant photoemission experiments which locate the  $d^8$  multiplets in these materials. [24] Looking at Fig. 1 of Ref. [23] we see that the  $d^8$  states occur in the energy range between 8 and 15 eV below the ZR singlet state. The large energy spread is due to the multiplet structure in the  $d^8$  configurations.

We now describe why the polarization dependence of these transitions will be very sensitive to where in momentum space the ZR states are situated and therefore the polarization dependence represents a test of the hypothesis described above. For this discussion the orthorhombic distortion is no longer important except for the proposal that it causes the doped hole states to be concentrated at the  $b$  minimum with a wave function given by

$$\psi_b(\mathbf{r}) = \chi(\mathbf{r}) \exp \left\{ i \frac{\pi}{2} x - i \frac{\pi}{2} y \right\}, \quad (11)$$

where  $\chi(\mathbf{r}) \propto e^{-\kappa r}$  is a relatively smooth wave function of the bound state,  $\kappa \approx 0.4$ . The smooth wave function is not important for optical absorption. Only the fast phase factor  $\exp \left\{ i \frac{\pi}{2} x - i \frac{\pi}{2} y \right\}$  is important. For a bound state based on a hole from the  $a$ -minimum the function  $\chi(\mathbf{r})$  is the same while the phase factor  $\exp \left\{ i \frac{\pi}{2} x + i \frac{\pi}{2} y \right\}$  is different.

To describe the above transition we clearly need to go beyond a  $t - J$  or Hubbard model taking into account explicitly the charge transfer nature of the gap as in the Zaanen-Sawatzky-Allen classification

scheme [25]. In Fig. 3 we display the  $\text{CuO}_2$  plane structure and the orbitals considered. The hole phase factor  $\exp \left\{ i \frac{\pi}{2} x - i \frac{\pi}{2} y \right\} = \pm 1, \pm i$  is shown in red near the corresponding Cu ion. The transition to a zero momentum ZR state is parity forbidden. However the hole resides in a ZR state with nonzero momentum where transition is optically allowed due to interference of ZR states centered on different Cu sites. Let us consider the case when the

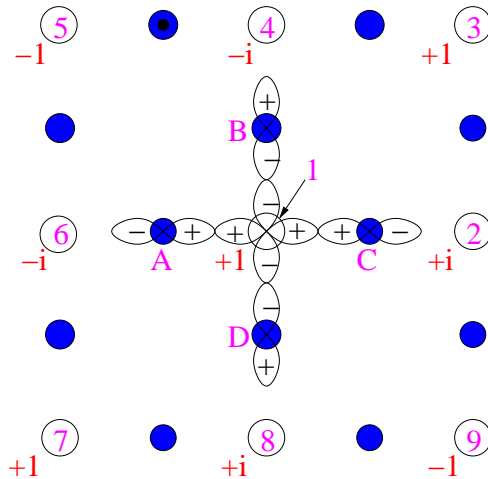


FIG. 3: (Color online)  $\text{CuO}_2$  plane. Open circles denote Cu ions and blue circles denote Oxygen ions. Cu ions in the cluster are enumerated by magenta numbers 1-9 and Oxygen ions are enumerated by four magenta letters A,B,C,D. The phase factor,  $\pm 1, \pm i$ , is shown in red near the corresponding Cu ion.

final hole resides at the first Cu site,  $|final\rangle = |\bar{d}_1\rangle$ . Here for short notations we denote  $d^8$  state as  $\bar{d}$ . The transition  $\bar{p} \rightarrow \bar{d}_1$  can occur when the initial p-hole resides on Oxygens A,B,C,D and comes from the ZR states centered at Cu sites 2,4,6,8. Therefore the transition amplitude is

$$A = \langle \bar{d}_1 | E_x x + E_y y | -i\bar{p}_A + i\bar{p}_C - i\bar{p}_B + i\bar{p}_D \rangle, \quad (12)$$

where  $\vec{E}$  is the electric field of the photon. Let us denote by  $D$  the dipole matrix element

$$\langle \bar{d}_1 | x | \bar{p}_C \rangle = D = \int \psi_{d_1} x \psi_{p_C} dV. \quad (13)$$

The symmetry relations between nonzero matrix elements follow from Fig. 3

$$\begin{aligned} \langle \bar{d}_1 | x | \bar{p}_A \rangle &= -D, \\ \langle \bar{d}_1 | y | \bar{p}_B \rangle &= D, \\ \langle \bar{d}_1 | y | \bar{p}_D \rangle &= -D. \end{aligned} \quad (14)$$

Hence, we find from (12)

$$A = 2i(E_x - E_y)D. \quad (15)$$

Thus we conclude that there is an absorption if the wave is polarized along the orthorhombic  $b$ -axis,  $\vec{E} \propto (1, -1)$

and there is no absorption if the wave is polarized along the orthorhombic  $a$ -axis,  $\vec{E} \propto (1, 1)$ . Basically this is the only possible correlation one can write kinematically,  $I \propto (\vec{E} \cdot \vec{k})^2$ , where  $\vec{k}$  is momentum of the hole. So, the answer is obvious even without a calculation. The optical absorption we have discussed is proportional to doping  $x$ . We stress that the prediction for the low temperature absorption asymmetry is  $\sigma_b \gg \sigma_a$  and this is equally applicable to the Neel and “spin-glass” phases of LSCO. The optical asymmetry is different from that in the dc conductivity where both experimentally [2] and theoretically [17] the asymmetry at low temperature is not that large,  $\sim 50\%$ , and of the opposite sign,  $\sigma_b < \sigma_a$ .

### IMPLICATIONS FOR ARPES

We consider photoemission from  $a$  and  $b$  nodal points. There is a difference in energy that is given by Eq. (10). This is already an interesting effect. However, there is a much bigger effect that is due to the spin spiral in the “spin-glass” phase. The pitch of the spiral directed along the  $b$ -axis is [8, 10]

$$\mathbf{Q} = \frac{gx}{\rho_s}(1, -1), \quad (16)$$

where  $\rho_s \approx 0.18J$  is spin stiffness,  $g \approx Zt \approx 0.7J$  is the hole-spin-wave coupling constant, and  $x$  is doping. Eq. (16) agrees very well with neutron scattering data. A hole with momentum  $\mathbf{q}$  interacts with the spiral. The interaction splits the hole dispersion in two branches with the following energy shift [8, 10]

$$\Delta\epsilon(\mathbf{q}) = \pm g|Q_x \sin q_x + Q_y \sin q_y|. \quad (17)$$

Thus the hole dispersion near the “ $a$ ” nodal point,  $\mathbf{q} \approx (\pi/2, \pi/2)$ , is practically not influenced by the spiral,  $\Delta\epsilon_a = 0$ . On the other hand the hole dispersion near the “ $b$ ” nodal point,  $\mathbf{q} \approx (\pi/2, -\pi/2)$ , is changed as

$$\Delta\epsilon_b = \pm \frac{2g^2x}{\rho_s}. \quad (18)$$

Accounting this correction together with (10) we find

$$\epsilon_b - \epsilon_a = -4Z\delta t' \pm \frac{2g^2x}{\rho_s} \sim -10 \pm 770x \text{ meV}. \quad (19)$$

Note that the second (collective) contribution of this difference scales linearly with doping and it is pretty large, it is  $\sim 30\text{meV}$  at  $x = 0.04$ .

Thus the present picture predicts that the lowest branch of the dispersion with energy approximately equal to chemical potential is at the nodal  $b$ -point. The dispersion at the nodal  $a$ -point is by  $\sim 40\text{meV}$  higher (we present the estimate for  $x = 0.04$ ). Finally, there is another branch of the dispersion at the nodal  $b$ -point that

is by  $\sim 60\text{meV}$  above the chemical potential, this branch can be pretty broad. The present consideration is applicable to the doping interval  $0.02 \leq x \leq 0.055$  where the disordered spiral is established. In the Neel phase,  $x \leq 0.02$ , the collective contribution in (19) is suppressed.

### CONCLUSIONS

We have demonstrated that the 0.9% orthorhombic distortion of the Cu lattice causes 7% difference in diagonal hopping matrix elements, and that the  $3^\circ$  tilting of the oxygen octahedra causes an additional 4% difference. This 11% difference together with the effect of strong magnetic fluctuations (small hole pockets) and together with localization of holes due to Coulomb trapping by Sr ions leads to depopulation of the  $(\pi/2, \pi/2)$  pocket in the insulating phase,  $x \leq 0.055$ . As a result the optical transition  $p^5d^9 \rightarrow p^6d^8$  is allowed only if the electric field is polarized along the orthorhombic  $b$ -axis.

Another prediction that is related to the spin spiral structure is the asymmetry of ARPES spectra: the hole dispersion at the  $b$ -nodal point is close to the chemical potential, while at the  $a$ -nodal point it is by 25-50 meV higher depending on doping.

- 
- [1] B. Keimer, A. Aharony, A. Auerbach, R. J. Birgeneau, A. Cassanho, Y. Endoh, R. W. Erwin, M. A. Kastner, and G. Shirane, Phys. Rev. B **45**, 7430 (1992). M. A. Kastner, R. J. Birgeneau, G. Shirane, and Y. Endoh, Rev. Mod. Phys. **70**, 897 (1998).
  - [2] Y. Ando, K. Segawa, S. Komiya, and A. N. Lavrov, Phys. Rev. Lett. **88**, 137005 (2002).
  - [3] M. Matsuda, M. Fujita, K. Yamada, R. J. Birgeneau, Y. Endoh, and G. Shirane, Phys. Rev. B **65**, 134515 (2002).
  - [4] S. Wakimoto, G. Shirane, Y. Endoh, K. Hirota, S. Ueki, K. Yamada, R. J. Birgeneau, M. A. Kastner, Y. S. Lee, P. M. Gehring, and S. H. Lee, Phys. Rev. B **60**, R769 (1999).
  - [5] M. Matsuda, M. Fujita, K. Yamada, R. J. Birgeneau, M. A. Kastner, H. Hiraka, Y. Endoh, S. Wakimoto, and G. Shirane, Phys. Rev. B **62**, 9148 (2000).
  - [6] M. Fujita, K. Yamada, H. Hiraka, P. M. Gehring, S. H. Lee, S. Wakimoto, and G. Shirane, Phys. Rev. B **65**, 064505 (2002).
  - [7] K. Yamada, C. H. Lee, K. Kurahashi, J. Wada, S. Wakimoto, S. Ueki, H. Kimura, Y. Endoh, S. Hosoya, G. Shirane, R. J. Birgeneau, M. Greven, M. A. Kastner, and Y. J. Kim, Phys. Rev. B **57**, 6165 (1998).
  - [8] O. P. Sushkov and V. N. Kotov, Phys. Rev. Lett. **94**, 097005 (2005).
  - [9] A. Lüscher, G. Misguich, A. I. Milstein, and O. P. Sushkov, Phys. Rev. B **73**, 085122 (2006).
  - [10] A. Lüscher, A. I. Milstein, and O. P. Sushkov, Phys. Rev. Lett. **98**, 037001 (2007).
  - [11] P. W. Anderson, Science **235**, 1196 (1987).

- [12] V. J. Emery, Phys. Rev. Lett. **58**, 2794 (1987).
- [13] F. C. Zhang and T. M. Rice, Phys. Rev. B **37**, R3759 (1988).
- [14] Y. Tokura, S. Koshihara, T. Arima, H. Takagi, S. Ishibashi, T. Ido, and S. Uchida, Phys. Rev. B **41**, R11657 (1990).
- [15] O. K. Andersen, A. I. Liechtenstein, O. Jepsen, and F. Paulsen, J. Phys. Chem. Solids **56**, 1573 (1995); E. Pavarini, I. Dasgupta, T. Saha-Dasgupta, O. Jepsen, and O. K. Andersen, Phys. Rev. Lett. **87** 047003 (2001).
- [16] M. Reehuis, C. Ulrich, K. Prokeš, A. Govar, G. Blumberg, Seiki Komiyama, Yoichi Ando, P. Pattison, and B. Keimer, Phys. Rev. B **73**, 144513 (2006).
- [17] V. N. Kotov and O. P. Sushkov, Phys. Rev. B **72**, 184519 (2005)
- [18] O. K. Andersen and T. Saha-Dasgupta, Phys. Rev. B **62**, R16219 (2000).
- [19] O. K. Andersen and O. Jepsen, Phys. Rev. Lett. **53**, 2571 (1984). The AS radii were 3.08, 2.15, 2.06 and 2.11  $a_0$  for respectively La, Cu,  $O_{x,y}$  and  $O_z$ . The ES radii were 2.22, 1.54, 1.30 and 1.22  $a_0$
- [20] P. Blaha, K. Schwarz, G. K. H. Madsen, D. Kvasnicka, and J. Luitz, *Wien2k*, ISBN 3-9501031-1-2.  $RK_{max}=7.5$ ,  $l_{max}=10$  and  $G_{max}=14$ . The MT radii were 2.29, 1.86, and 1.65  $a_0$  for respectively La, Cu, and O.
- [21] TABLE II in O.K. Andersen, W. Klose, and H. Nohl, Phys. Rev. B **17**, 1209 (1978).
- [22] T. Saha Dasgupta, J. Nuss, and O.K. Andersen, unpublished.
- [23] H. Eskes and G. A. Sawatzky, Phys. Rev. Lett. **61**, 1415 (1988).
- [24] L. H. Tjeng, C. T. Chen, and S. W. Cheong, Phys. Rev. B **45**, 8205 (1992).
- [25] J. Zaanen, G. A. Sawatzky and J.W. Allen, Phys. Rev. Lett. **55**, 418 (1985).